Russian Physics Journal, Vol. 53, No. 9, 2011

A PHYSICAL MODEL OF DIELECTRIC SPECTRA OF THAWED AND FROZEN BENTONITIC CLAY WITHIN THE FREQUENCY RANGE FROM 1 TO 15 GHZ

V. L. Mironov[1] and Yu. I. Lukin[2]

UDC 621.371.3

The dielectric spectra of moist specimens of bentonitic clay are measured within the frequency range from 1 to 15 GHz at positive and negative temperatures. The phase transitions in different types of water present in the clay specimen are investigated in the process of its freezing. The parameters of dielectric relaxation and conductivity of different water types in the specimen are determined. A thermal dielectric model for thawed and frozen bentonitic clay is developed.

Keywords: dielectric spectra, moist specimens, bentonitic clay, microwaves, phase transitions.

INTRODUCTION

Inorganic soils constitute a significant part of the soil cover, making it critical to take their dielectric properties into consideration in the subsurface radio remote sensing. Of special interest is the soil water phase transition during soil freezing – thawing in the course of seasonal temperature variations. This work presents the results of measurements of the complex dielectric permittivity (CDP) of inorganic soil, using moist bentonitic clay as an example. Some results on the study of dielectric properties of moist bentonitic clay were published by us earlier. In particular, in [1] we found out that the dependence of the CDP of bentonite on the water content (moisture) can be described by a refractive mixing formula and reported the presence of soil water in free and bound states. The refractive mixing model allowed us to determine the maximum gravimetric fraction of bound water (MGFBW). Further, that model was extended to become a generalized refractive mixing dielectric model (GRMDM) [2] when we took into consideration the frequency dependence of the soil water CDP, which was determined by the Debye model, with its spectroscopic parameters being measured. In [3], the GRMDM was complimented with thermal dependeces of spectroscopic parameters, and a thermal GRMDM was proposed in the case of soil rich in organic matter.

In this work we developed a thermal GRMDM for the bentonitic clay, taking into account both thawed and frozen conditions. In addition to the bound and free types of soil water earlier identified [2], we discovered a third type of water – transient water, also referred to as film water [4]. The film (or transient) water is less subjected to surface forces than bound water is. The former is held near mineral surfaces by much weaker forces. We found the parameters of the thermal GRMDM for all the tree types of water in bentonite. Thus, this work improve the current GRMDM, by taking into account the soil water phase transitions in the course of freezing, and refines the concept of the physical state of water in this soil type.

[1]L. V. Kirenskii Institute of Physics of the Siberian Branch of the Russian Academy of Sciences, Krasnoyarsk, Russia, [2]M. F. Reshetnev Siberian State Aerospace University, Krasnoyarsk, Russia, e-mail: rsdvm@ksc.krasn.ru.
Translated from Izvestiya Vysshikh Uchebnykh Zavedenii, Fizika, No. 9, pp. 71–76, September, 2010. Original article submitted June 24, 2010.

CONCEPT OF THE THERMAL GRMDM

According to GRMDM [2], the dielectric permittivity (DP) ε' and dielectric loss factor (LF) ε″ are calculated by the formulas

$$\varepsilon' = n^2 - \kappa^2,\ \varepsilon'' = 2n\kappa,\ n^* = \sqrt{\varepsilon} = n + i\kappa,\ \varepsilon = \varepsilon' + i\varepsilon'', \tag{1}$$

where ε and n^* are the CDP and the complex index of refraction (CIR), n is the index of refraction (IR), and κ is the normalized attenuation coefficient (NAC).

In accordance with [3], the reduced CIR of moist soil is expressed via the CIRs of bound water, film water, liquid capillary (free) water, and icy capillary water using the refractive mixing formula as follows:

$$\begin{aligned}\frac{n_s^*(m_g,f,t)-1}{\rho_d(m_g)} &= \frac{\left(n_m^*-1\right)}{\rho_m} + \frac{\left(n_b^*(m_g,f,t)-1\right)}{\rho_b}[m_g + (m_{g1}-m_g)u(m_g-m_{g1})] \\ &+ \frac{\left(n_f^*(m_g,f,t)-1\right)}{\rho_f}[(m_g-m_{g1})u(m_g-m_{g1}) + (m_{g2}-m_g)u(m_g-m_{g2})] \\ &+ \frac{\left(n_u^*(m_g,f,t)-1\right)}{\rho_u}(m_g-m_{g2})u(m_g-m_{g2}),\end{aligned} \tag{2}$$

where ρ stands for the density of bulk soil and soil components, the subscripts, s, d, m, b, f, and $u = u$ or $u = i$ are attached to the values n^* and ρ in order to designate moist soil, dry soil, soil solids, bound water, film water, and capillary liquid water ($u = u$) or icy water ($u = i$), respectively, m_g is the gravimetric moisture (ratio of mass of soil water to mass of dry soil), and m_{g1} is the maximum gravimetric fraction of bound water (MGFBW), m_{g2} is the transition moisture which separates the range of capillary liquid water or icy water, $m_g > m_{g2}$, from that of film water, $u(x)$ is the Heaviside step function: $u(x) = 1$ if $x > 0$, and $u(x) = 0$ if $x \le 0$. The term $(n_m^* - 1)/\rho_m$ is a reduced CIR of the soil solids, and we consider this entire term as a single material property of the soil solids.

The refractive mixing model (2) determines the dependence of the CIR on moisture as a chain function. The break points correspond to a transition from one water type to another as the total water content in the specimen is increased. The real and imaginary parts of the CIR for all the types of soil water are related to the DP and the LF as follows:

$$n_p = \frac{1}{\sqrt{2}}\sqrt{\sqrt{\varepsilon'^2_p + \varepsilon''^2_p} + \varepsilon'^2_p}, \tag{3}$$

$$\kappa_p = \frac{1}{\sqrt{2}}\sqrt{\sqrt{\varepsilon'^2_p + \varepsilon''^2_p} - \varepsilon'^2_p}. \tag{4}$$

where subscript p can be replaced by any subscript attached to n^* or ρ in formula (2)

The CDP spectra for all of the water types are given by the Debye formulas

$$\varepsilon'_p = \varepsilon_{\infty p} + \frac{\varepsilon_{0p} - \varepsilon_{\infty p}}{1 + (2\pi f \tau_p)^2}, \tag{5}$$

$$\varepsilon''_p = \frac{\varepsilon_{0p} - \varepsilon_{\infty p}}{1 + (2\pi f \tau_p)^2} 2\pi f \tau_p + \frac{\sigma_p}{2\pi \varepsilon_r f}, \tag{6}$$

where ε_{0p} is the low-frequency limit of dielectric permittivity, $\varepsilon_{\infty p}$ is the high-frequency limit of dielectric permittivity, τ_p is the effective molecule relaxation time, σ_p is the ionic conductivity of soil water solution, and $\varepsilon_r = 8.854 \cdot 10^{-12}$ F/m is the dielectric permittivity of vacuum. The low-frequency limit of dielectric permittivity ε_{0p} as a function of temperature is expressed by the Clausius–Massotti formula [3].

$$\varepsilon_{0p}(T) = \frac{1 + 2\exp\left[F_{0p}(t_{s\varepsilon 0p}) - \beta_{0p}(t - t_{s\varepsilon 0p})\right]}{1 - \exp\left[F_0(t_{s\varepsilon 0p}) - \beta_{0p}(t - t_{s\varepsilon 0p})\right]}, \tag{7}$$

where β_{0p} is the is the coefficient of volumetric expansion (1/K) and t and $t_{s\varepsilon 0p}$ are the current and starting temperatures (°C). Function $F_{0p}(t)$ can be given by

$$F_{0p}(t) = \ln\left[\frac{\varepsilon_{0p}(t) - 1}{\varepsilon_{0p}(t) + 2}\right]. \tag{8}$$

The high frequency limit $\varepsilon_{\infty p}$ is assumed to be independent of the temperature and equal to 4.9, according to [2]. For the temperature dependence of the relaxation time, we used the following formula:

$$\tau_p = \frac{48}{TK}\exp\left[\frac{\Delta H_p}{R}\frac{1}{TK} - \frac{\Delta S_p}{R}\right] \tag{9}$$

where the value of τ_p is given in picoseconds, ΔH_p is the activation energy of the relaxation process (J/mol), ΔS_p is the activation entropy of the relaxation process (J/(mol·K)), T_K is the temperature (K), and R is the universal gas constant ((J/(mol·K)).

Conductivity σ_p follows a linear dependence on temperature as do ionic solutions

$$\sigma_p(t) = \sigma(t_{s\sigma p}) + \beta_{\sigma p}(t - t_{s\sigma p}) \tag{10}$$

where $\beta_{\sigma p}$ is the derivative of conductivity with respect to temperature (S/m·K), $\sigma_p(t_{s\,\sigma p})$ is the value of conductivity (S/m) at the starting temperature $t_{s\,\sigma p}$(°C).

RESULTS AND DISCUSSION

Measurement of the CDP spectra of bentonitic clay within the frequency range from 1 to 16 GHz, the moisture range from 0 to 0.9 g/g, and the temperature range from от +25 to –20°C allowed us to find the GRMDM parameters, that is, ε_{0p} ,$\varepsilon_{\infty p}$, τ_p, σ_p, $(n^*_m\text{-}1)/r_m$, m_{g1}, and m_{g2} as a function of temperature, using the technique proposed in [2] and [3]. According to the GRMDM concept, the dependence of the reduced IRs and NACs is a chain function of soil moisture as given by (2). It is evident from Figs. 1 and 2 that this dependence is valid for the bentonitic clay measured. On the other hand, in contrast to previous measurements [2], [3], two breakpoints are clearly identified at the moistures $m = m_{g1}$ and $m = m_{g2}$, and hence tree water types can be indicated. We further refer to those as the bound ($m < m_{g1}$), capillary liquid water or icy water ($m > m_{g2}$), and film water ($m_{g1} < m < m_{g2}$).

It follows from Eq. (2) and Fig. 2, for the specimen moisture $m_g > m_{g2}$ and at $t < -$ 8ºC, that the slope ratios of the reduced IR with respect to the moisture axis are close to the values corresponding to the reduced IR of ice, and these are only slightly dependent on temperature, with the linear dependences for different temperatures being nearly parallel. This implies a conclusion that capillary water at $t < -$ 8ºC turns into icy water.

A different pattern is observed for the moisture ranges $m_{g1} < m_g < m_{g2}$: and $m_g < m_{g1}$: in these cases, the slope ratios of the reduced IR to the moisture axis do depend on frequency and exceed the values for ice, and with the

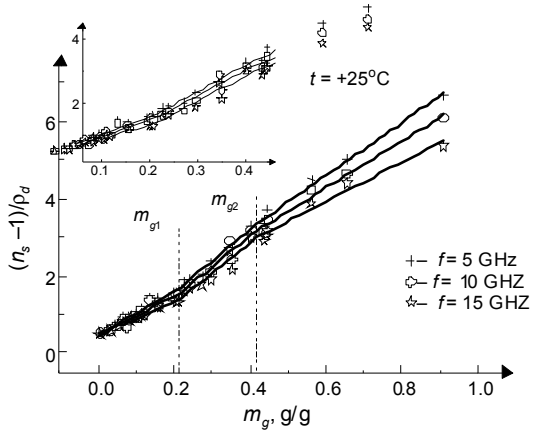

Fig. 1

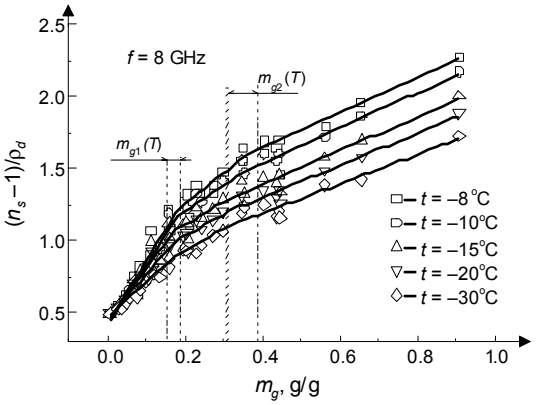

Fig. 2

Fig. 1. Dependence of the reduced index of refraction $(n_s - 1)/\rho_d$ on moisture at the temperature 25ºC and the frequencies 5, 10, and 15 GHz. The solid lines are the fits attained with the refractive mixing model formula (2).

Fig. 2. Dependence of the reduced index of refraction $(n_s - 1)/\rho_d$ on moisture at the negative temperatures (idicated in the legend) and the frequency 8 GHz. The solid lines are the fits obtained with the refractive mixing model formula (2)

temperature decreasing they tend to the values typical for ice. Thus, a conclusion can be drawn that the bound ($m_g < m_{g1}$) and film ($m_{g1} < m_g < m_{g2}$) water in bentonitic clay form nonfreezing water as the temperature drops below –8°C.

By the regression analysis of the measured dependences on the moisture for the reduced IR and NAC of the bentonitic clay, which was conducted for the temperature interval from – 30 to +25ºC and the frequency range from 1 to 15 GHz, and using Eq. (2) we obtained the temperature dependences for the reduced IR and NAC of the soil solids (Fig. 3).

It is clear from Fig. 2 that the values of the MGFBW m_{g1} and the sum of maximum gravimetric fractions of bound and film types of water (MGFBFW) m_{g2} vary with temperature. In order to identify the pattern of this variation, in Fig. 4 we separately present the temperature dependences $m_{g1}(t)$ and $m_{g2}(t)$. The regression formulas for the temperature dependences of these parameters are given by

$$m_{g1} = \begin{cases} 0.20 + 3.28 \cdot 10^{-5} \exp(-t / 0.89), & -8^{\circ}\mathrm{C} < t < 25^{\circ}\mathrm{C}, \\ 0.17 + 1.29 \exp(t / 1.95), & -30^{\circ}\mathrm{C} < -8^{\circ}\mathrm{C}, \end{cases} \tag{11}$$

$$m_{g2} = \begin{cases} 0.42 + 6.56 \cdot 10^{-4} \exp(-t/1.73), & -8^{\circ}\mathrm{C} < t < 25^{\circ}\mathrm{C}, \\ 0.31 + 1.04 \exp(t/2.91), & -30^{\circ}\mathrm{C} < -8^{\circ}\mathrm{C}, \end{cases} \tag{12}$$

In Fig. 4, both the MGFBW and MGFBFW are seen to sharply decrease as the temperature drops below −8°C. This behavior implies for the film water to be gradually (by infinitesimal portions) turning into icy water, with its amount simultaneously increasing at the expense of the bound water. On the other hand, it is evident from Figs. 2 and 4 that this kind of mass exchange is almost terminated at t = –15ºC, and the weight content of both water types remains constant when the temperature further decreases, which is indicative of the fact that there exists a residual mass of nonfreezing water within the temperature interval from about –30 to –15ºC.

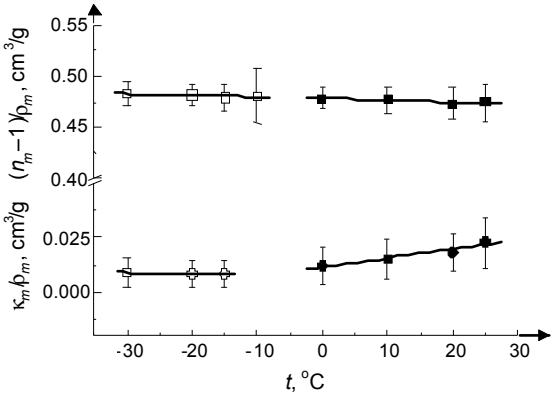

Fig. 3

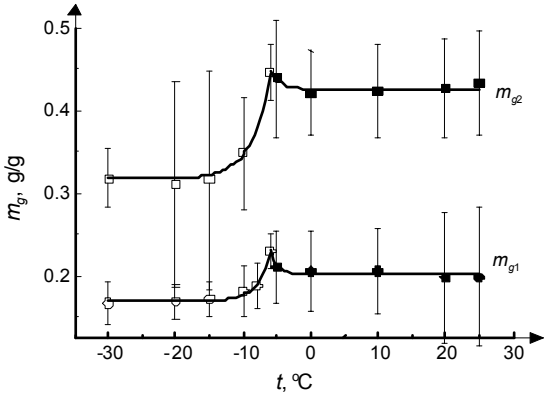

Fig. 4

Fig. 3. Temperature dependence of the reduced IR $(n_m - 1)/\rho_m$ and NAC κ_m / ρ_m of the soil solids.

Fig. 4. Temperature dependence of the MGFBW m_{g1} and MGFBFW m_{g2}.

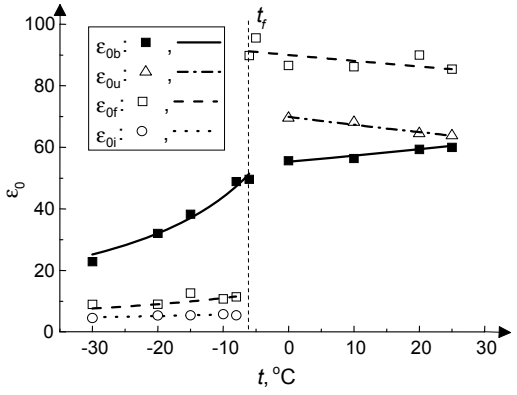

Fig. 5

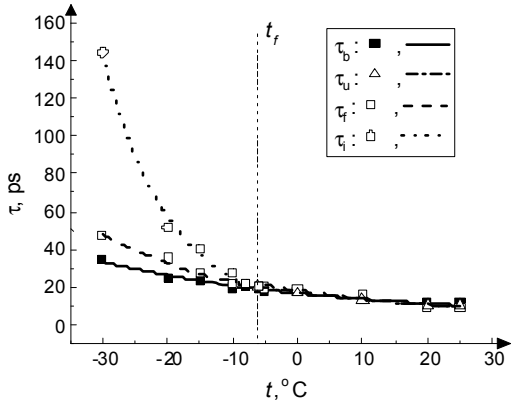

Fig. 6

Fig. 5. Temperature dependence of the low-frequency limit of DP of the bound ε_{0b}, film ε_{0f}, capillary liquid ε_{0u} and icy water ε_{0i}.

Fig. 6. Temperature dependence of the relaxation time of the bound τ_b, film τ_f, capillary liquid τ_u, and icy τ_i water.

The temperature dependence of the spectroscopic parameters of the GRMDM for all types of water contained in the bentonitic clay is given in Figs. 5–7. An analysis of Fig. 5 shows that the low-frequency limit of the DP of film and capillary water types at the temperature of liquid capillary water phase transition, which is about −8°C, change their values abruptly, while in the case of bound water this value appears to decrease as a continuous function.

The relaxation time dependences for specific types of soil water, presented in Fig. 6, differ from each other to a large extend in the case of frozen specimens. It should be noted that the relaxation times, corresponding to all the water types in frozen specimens, increase with decreasing temperature, which may take place due to their molecular structure rearranging towards that of ice. In frozen specimens, the relaxation time of film water behaves as that of the bound water.

TABLE 1

Water type	$\varepsilon_{0p}(t_{sp})/t_{sp}$	$\varepsilon_{\infty p}(t)$	β_{0p}, K^{-1}	$\Delta H_p/R$, K^{-1}	$\Delta S_p/R$	$\sigma(t_{s\sigma p})/t_{s\sigma p}$ S/m	$\beta_{\sigma p}/t_{s\sigma p}$ S/(m·K)
Capillary liquid water, $p = u$, $-8°C < t < 25°C$	63.8/25ºC	4.9	$1.6\cdot10^{-4}$	1612	1.32	1.13/ 20°C	0.020
IcY Water $p = i$, $-30°C < t < -8°C$	5.43/ –15ºC	4.0	$-4.3\cdot10^{-3}$	5401	15.60	0.07/–10°C	0.004
Film water, $p = f$, $-8°C < t < 25°C$	85/25ºC	4.9	$7.0\cdot10^{-5}$	1864	2.19	4.30/25°C	0.098
Film water, $p = f$, $-30°C < t < -8°C$	9.023/ –20ºC	4.9	$-5.6\cdot10^{-3}$	2008	2.79	0.15/ –20°C	0.006
Bound water, $p = b$, $-8°C < t < 25°C$	59/20ºC	4.9	$-1.8\cdot10^{-4}$	1269	0.09	3.80/20°C	0.089
Bound water, $p = b$, $-30°C < t < -8°C$	35/ –15ºC	4.9	$-2.5\cdot10^{-3}$	1271	0.10	0.98/ –20°C	0.027

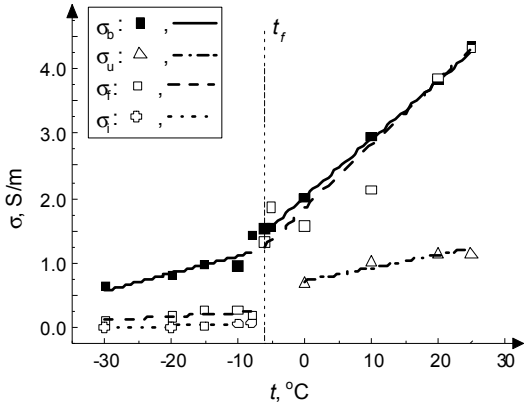

Fig. 7. Temperature dependence of conductivity of the bound σ_b, film σ_f, liquid capillary σ_u, and icy water σ_i types.

Shown in Fig. 7 are the temperature dependences of conductivity for the bound, film, liquid capillary, and icy water types. As seen from Fig. 7, for all the water types, there is a discontinuity in conductivity at the temperature of soil specimens freezing $t = -8°C$.

As a result of regression analysis, using the data given in Figs. 5 to 7 alongside with the formulas (7)–(10), we obtained the parameters of the thermal GRMDM for the bentonitic clay under study, which are summarized in Table 1.

In order to test the temperature dependent dielectric model, we constructed the dependences of the measured DPs and LFs of moist bentonitic clay versus those calculated with the model, which are shown in Figs. 8 and 9, using the formulas (1)–(10) and the data from Table 1. The solid lines in the plots correspond to the 1 to 1 dependences between the measured and simulated values, the dotted lines are the linear regression dependences:

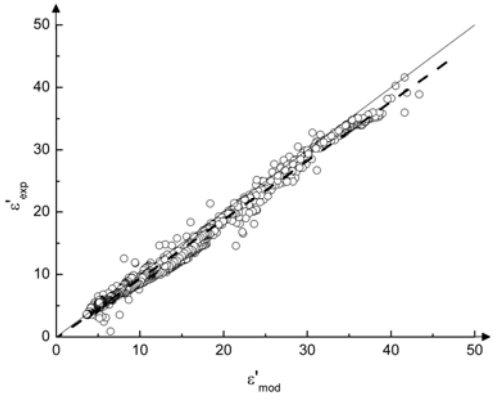

Fig. 8

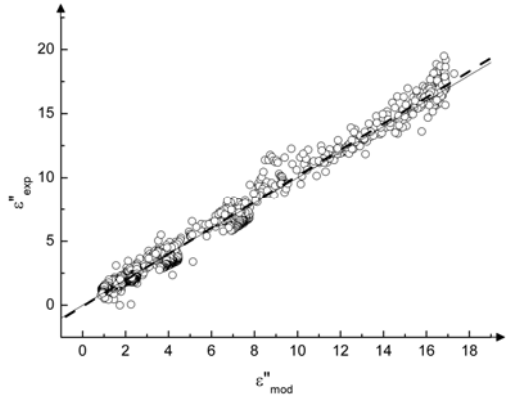

Fig. 9

Fig. 8. Correlation between the measured and simulated data on ε' of moist bentonitic clay for the temperatures from − 20ºC to +25, frequencies from 1 to 15 GHz, and moistures m_g = 0.11, 0.24, 0.30, and 0.91 g/g.

Fig. 9. Correlation between the measured and simulated data on ε" of moist bentonitic clay for the temperatures from − 20ºC to +25, frequencies from 1 to 15 GHz, and moistures m_g = 0.11, 0.24, 0.30, and 0.91 g/g.

$\varepsilon'_{exp} = -0.18 + 0.95\varepsilon'_{mod}$ and $\varepsilon''_{exp} = -0.08 + 1.02\varepsilon''_{mod}$, for the dielectric permittivity and loss factor, respectively. The correlation coefficient between the measured and simulated values was found to be 0.99 for DP and LF. The standard deviation between the measured and simulated values appeared to be 0.89 for DP and 0.60 for LF.

SUMMARY

We have measured the CDP spectra of moist bentonitic clay, as an example of inorganic soil, within the frequency range from 1 to 15 GHz and in the temperature range from – 30 to +25ºC, in a cycle of freezing the soil specimens.

We have discovered the presence of four water types in this soil: bound, film, liquid capillary, and icy. It has been shown that the bound and film water types constitute the nonfreezing water. The mass exchange between the nonfreezing bound and nonfreezing film water types has been investigated, as well as that between the nonfreezing film water and icy water. It has been found out that at –20ºC the mass exchange is mostly terminated and the weight content proportions between different water types (bound nonfreezing, film nonfreezing, and icy) present in a frozen soil specimen remain unchanged. This means that, in contrast to the common conceptions [6, 7], there exists a certain amount of residual nonfreezing water that does not transfer into ice by infinitesimally small portions (i.e., it does not get "frozen off"), when the temperature of the frozen specimen is decreased. Though the dielectric properties of the residual nonfreezing water types tend to those of icy water when the temperature decreases, this takes place most likely due to changing in their molecular structure.

Also, the parameters of the thermal GRMDM have been introduced and derived from the dielectric data measured. The error of the thermal GRMDM has been tested, and the coefficient of correlation between the measured and modeled values of the CDPs of moist clay specimens has been found to be 0.99 for both DP and LF.

This study has been supported by the Complex integration project of the SB RAS Presidium, Grant No. 6 and a joint RFBR – France grant No. 09-05-91061-NTSNI.

REFERENCES

1. V. L. Mironov, S. A. Komarov, and V. N. Kleshchenko, Proc. IGARSS'05, Seoul, Korea, 3196–3199 (2005).
2. V. L. Mironov, M. C. Dobson, V. H. Kaupp, *et al*., IEEE Trans. Geosci. Remote Sensing, **42**, No. 4, P. 773–785 (2004).
3. V. L. Mironov, R. D. De Roo, I. V. Savin, *Ibid*., 48, No. 6, 2544–2556 (2010).
4. V. T. Trofimov *et al*., Soil Study [in Russian], Moscow, Nauka (2005).
5. S. A. Komarov, V. L. Mironov, and Yu. I. Lukin, Russ. Phys. J., No. 9, 934–939 (2006).
6. Lithogenic Geocryology. Part II [in Russian] (Ed. E. D. Ershov), Moscow, MSU Publishers (1986).
7. E. D. Ershov, Physics, Chemistry and Mechanics of Frozen Rocks [in Russian], Moscow, MSU Publishers (1986).